Effect of Carboxyl Graphene on Direct Electrochemistry of Myoglobin and Electrocatalytic Investigation

Wen Zheng[1,2], Wenshu Zhao[1], Wei Chen[1,2], Wenju Weng[1,2], Zhengwei Liao[1], Ruixia Dong[1], Guangjiu Li[2], Wei Sun[1,]*

[1] Key Laboratory of Tropical Medicinal Plant Chemistry of Ministry of Education, College of Chemistry and Chemical Engineering, Hainan Normal University, Haikou 571158, P R China
[2] College of Chemistry and Molecular Engineering, Qingdao University of Science and Technology, Qingdao 266042, PR China
[*]E-mail: swyy26@hotmail.com

In this paper the effect of carboxyl graphene (G-COOH) on the electrochemical behavior of myoglobin (Mb) was investigated in detail. A Nafion, Mb and G-COOH modified carbon ionic liquid electrode (CILE) was constructed and applied to electrochemical biosensing. G-COOH with high conductivity and good biocompatibility could act as an electron transfer bridge for enhancing the electron transfer reactivity of Mb. In phosphate buffer solution (pH 6.0) Mb exhibited a pair of good-shape redox peaks on cyclic voltammogram with the formal peak potential ($E^{0'}$) as -0.255 V (vs. SCE). Electrochemical studies of Mb were checked with electrochemical parameters calculated. Mb molecules on the electrode displayed excellent electrocatalytic reduction to trichloroacetic acid (TCA). The current showed a linear response to TCA concentrations from 5.0 to 57.0 mmol L^{-1} with a low detection limit (1.0 mmol L^{-1}). The Michaelis–Menten constant (K_M^{app}) of the fabricated Mb bioelectrode for TCA was determined as 1.30 mmol L^{-1}. Therefore the usage of G-COOH established an effective platform for direct electrochemistry of redox enzymes in the field of third-generation electrochemical sensor.

1. INTRODUCTION

Direct electron transfer from redox enzymes to electrode has been widely studied in past decades [1]. The results can be used to know the electron transfer mechanisms in biomolecules, biological system or biocatalytic process. Also the model can be applied to the construction of bioreactors and biosensors [2, 3]. As a commonly used redox protein with one

iron heme inside the polypeptide chain, myoglobin (Mb) has been selected as the model for the electrochemical investigation [4]. However, electron transfer of Mb in solution or naked solid electrode is at slow rate with unstable responses, which is ascribed to the deep burying of electroactive center inside the protein structure [5]. Therefore many reports had been focused on nanomaterials modified electrodes to improve the electron transfer efficiency [6, 7].

Graphene (GR) is a two-dimensional carbon nanosheet which has specific physicochemical properties including big surface area, good optical transparency, high conductivity and mechanical strength. GR has excellent electrochemical conductivity with certain electrocatalytic ability, which had been used in electrochemical sensors and modified electrodes [8-10]. It had been proved that GR based electrochemical sensors exhibited better performances than other nanomaterial based sensors [11]. Recently carboxyl functionalized GR had attracted intense attentions. The presence of carboxyl group can modify the interfacial properties of GR, increase the hydrophilicity and decrease the stacking effect of GR nanosheets. Therefore carboxyl groups on the surface of GR led to a great effect on structure and functions [12, 13]. Also the carboxyl group can be further derived and reacted with other functional groups by amidation or esterification for the preparation of functionized GR composite [14].

In the present work, the effect of carboxyl graphene (G-COOH) on the electrochemistry of Mb was checked with Nafion film for immobilization. Nafion can form a stable film and fix the composite on the electrode tightly. The Mb-G-COOH mixture was casted on the surface of CILE with Nafion film and direct electrochemistry of Mb was investigated. The Mb-G-COOH based electrode exhibited good electrocatalytic activity to the reduction of trichloroacetic acid (TCA), indicating the successful fabrication of third-generation electrochemical biosensor.

2. EXPERIMENTAL

2.1 Reagents

Mb (MW. 17800, Sigma-Aldrich Co., USA), 1-hexylpyridinium hexafluorophosphate (HPPF$_6$, Lanzhou Yulu Fine Chemical Ltd. Co., China), graphite powder (particle size 30 μm, Shanghai Colloid Chem. Co., China), Nafion (5% ethanol solution, Sigma), TCA (Tianjin Kemiou Chemical Ltd. Co., China) and G-COOH (Nanjing XFNANO Materials Tech. Ltd. Co., China) were used as received. 0.1 mol L^{-1} phosphate buffer solutions (PBS) were used with other analytical reagent grade chemicals and doubly distilled water used throughout.

2.2 Apparatus

Cyclic voltammetry and electrochemical impedance spectroscopy (EIS) were performed on CHI 1210A and CHI 660D electrochemical analyzer (Shanghai Chenhua Instrument, China). A three-electrode model was employed with a modified CILE working electrode, a platinum wire auxiliary electrode and a saturated calomel reference electrode (SCE). Spectra were performed on Nicolet 6700 FT-IR spectrophotometer (Thermo Fisher Scientific Inc., USA) and TU-1901 double beam UV-Visible

spectrophotometer (Beijing General Instrument Ltd. Co., China). The image of scanning electron microscopy (SEM) was on a JSM-7100F scanning electron microscope (Japan Electron Co., Japan).

2.3 Preparation of Nafion/Mb-G-COOH/CILE

CILE was home-made as described previously with $HPPF_6$ as the binder [15], which was polished carefully to obtain a mirror-like surface before use. The composite was got by mixing a solution containing 15.0 mg mL^{-1} Mb and 1.0 mg mL^{-1} G-COOH. Then 6.0 μL of Mb-G-COOH mixture was casted on CILE surface and dried slowly. At last 8.0 μL of 0.5% Nafion solution was dropped on the electrode with a stable film formed, which was named as Nafion/Mb-G-COOH/CILE and put in a 4°C refrigerator. Other working electrodes were also made by the similar procedures for comparison.

2.4 Electrochemical measurements

Electrochemical measurements were performed in a 10.0 mL cell with PBS as the supporting electrolyte, which was deoxygated with purified N_2 for 0.5 h before the experiments with a N_2 environment kept in the experiments. UV-Vis absorption spectroscopy was recorded with a mixture solution of Mb and G-COOH by scanning from 300 nm to 600 nm. The Mb-G-COOH mixture was dropped on a glass slide and air-dried to get the sample for FT-IR experiment, which was scraped and tableted with KBr power.

3. RESULTS AND DISCUSSION

3.1 Characterization of G-COOH and its mixture with Mb

SEM image of G-COOH was shown in Fig. 1A, which gave the typical wrinkled like surface morphology and the large surface area could be used for the loading of redox proteins. UV-Vis absorption spectroscopy is used to probe the structural information of proteins. The Soret absorption band can prove the denaturation or the conformational changes of the protein heme region [16]. As shown in Fig. 1B, UV-Vis absorption spectra of Mb in water (curve a) and Mb-G-COOH mixture (curve b) had the same Soret band at 409.0 nm, indicating that Mb was not denatured after mixing with G-COOH due to its good biocompatibility with plenty of carboxyl group. FT-IR spectroscopy is another technique to probe the tertiary structure of proteins with amide I and II infrared bands [17]. The amide I band (1700–1600 cm^{-1}, C=O stretching vibration of peptide linkages) and the amide II band (1625–1500cm^{-1}, the combination of N–H bending and C–N stretching vibration in the backbone of protein) were shown in Fig. 1C and D. Two amide bands of Mb (Fig. 1C) appeared at 1646.9 cm^{-1} and 1537.0

cm[-1], which were close to those of Mb-G-COOH at 1647.0 cm^{-1} and 1545.4 cm^{-1} (Fig. 1D). Therefore the structure of Mb kept unchanged after mixed with G-COOH.
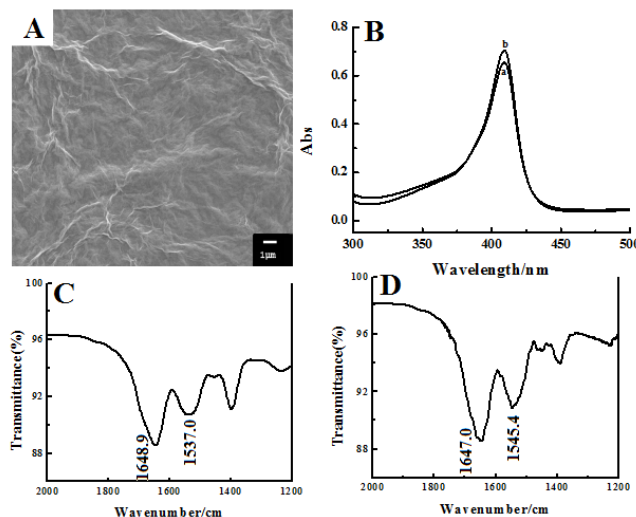

Figure 1. (A) SEM images of G-COOH; (B) UV-Vis absorption spectra of (a) Mb and (b) G-COOH-Mb in water; FT-IR spectra of (C) Mb and (D) Mb-G-COOH film.
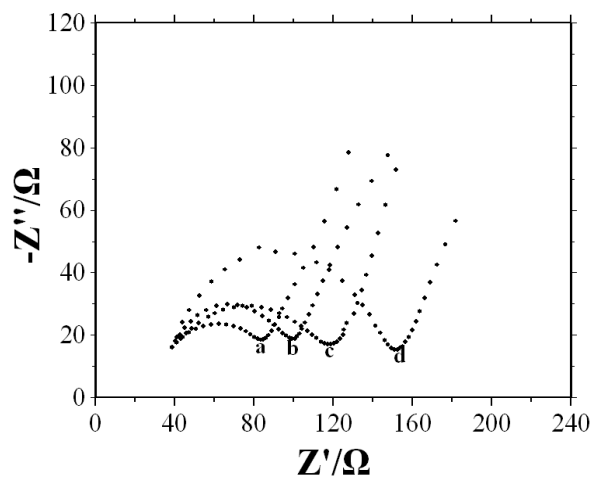
3.2 EIS results

Figure 2. EIS of (a) Nafion/Mb-G-COOH/CILE, (b) CILE, (c) Nafion/CILE and (d) Nafion/Mb/CILE in a 10.0 mmol L^{-1} $[Fe(CN)_6]^{3-/4-}$ and 0.1 mol L^{-1} KCl solution with the frequencies swept from 10[4] to 0.1 Hz.

EIS is applied to monitor the modification process on the interface. In EIS the semicircle part at higher frequencies is related to the electron transfer limited process with the diameter equals to the electron transfer resistance (Ret). The Ret value represents the electron transfer kinetics of the redox probe on the electrode. Fig. 2 gave the impedance spectra of Nafion/Mb-G-COOH/CILE (curve a), CILE (curve b), Nafion/CILE (curve c) and Nafion/Mb/CILE (curve d), which was recorded at the

open circuit potential in a 10.0 mmol L^{-1} [Fe(CN)$_6$]$^{3-/4-}$ and 0.1 mol L^{-1} KCl solution. Compared to Ret value of CILE (81.926 Ω, curve b), that of Nafion/CILE (116.754 Ω, curve c) became bigger, which was due to the nonconductive Nafion film obstructed the electron transfer. The immobilization of Mb further resulted in an obvious increase of the interfacial resistance (130.540 Ω, curve d), demonstrating that Mb was fixed on the electrode. With the further addition of G-COOH into Nafion/Mb/CILE, semicircular diameter became smaller with Ret value as 71.725 Ω (curve a), indicating that high conductive G-COOH could decrease the interfacial electron transfer resistance.

3.3 Direct electrochemistry of Mb modified electrode

Fig. 3 showed cyclic voltammograms of different modified electrodes in deaerated 0.1 mol L^{-1} pH 6.0 PBS with scan rate as 100 mV s^{-1}. No redox responses could be found on Nafion/G-COOH/CILE (curve a), CILE (curve b), and Nafion/CILE (curve c). On Nafion/Mb-G-COOH/CILE (curve d) a pair of well-shaped and nearly symmetrical redox peaks was observed, which was due to the realization of direct electron transfer of Mb. Therefore G-COOH on the electrode could increase the adsorption amount for Mb, favor the orientation of Mb on the surface and fast the electron transfer rate. The cathodic (Epc) and anodic (Epa) peak potential appeared at -0.296 V and -0.213 V with the formal peak potential (E$^{0'}$, defined as the average of Epa and Epc) as -0.255 V (vs. SCE), which was the characteristic of Mb heme Fe(III)/Fe(II) redox couple. The separation of peak potentials (ΔE$_p$) was 83 mV at the scan rate of 100 mV s^{-1} and almost unchanged with the increase of scan rate. Also the ratio of Ipc to Ipa was close to one. These date indicated that Mb took place a quasi-reversible electrochemical process on Nafion/Mb-G-COOH/CILE.
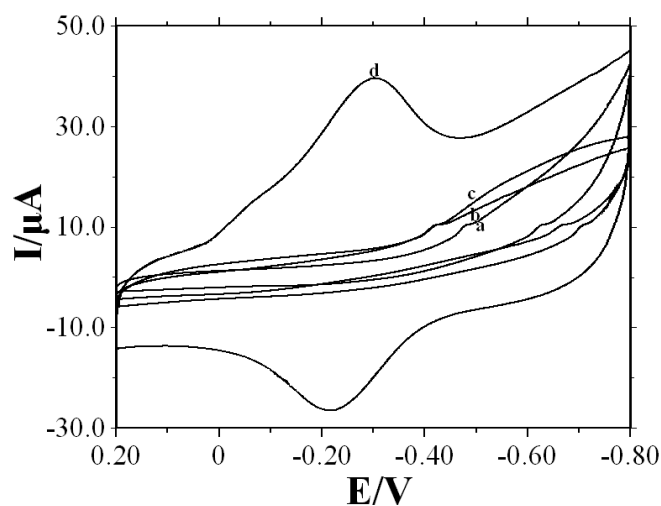

Figure 3. Cyclic voltammograms of (a) Nafion/G-COOH/CILE, (b) CILE, (c) Nafion/CILE and (d) Nafion/Mb-G-COOH/CILE in pH 6.0 PBS at the scan rate of 100 mV s^{-1}.

3.4 Electrochemical investigations

The effect of scan rate on direct electrochemistry of Nafion/Mb-G-COOH/CILE was checked checked from 40 to 1000 mV s^{-1} with the curves shown in Fig. 4A. A pair of symmetrical redox peaks with almost same value appeared at the same scan rate with the shift of the redox peak potential. The redox peak currents (Ip) increased with scan rate and two linear regression equations were calculated as Ipc (μA) =125.82υ (V s^{-1}) + 4.81 (n=10, γ=0.997) and Ipa (μA) =-126.51υ (V s^{-1})-6.37 (n=10, γ=0.998) (Fig. 4B), respectively. These results proved a typical surface-controlled thin-layer electrochemical process. According to the equation ($\Gamma^*=Q/nAF$) [18], the surface concentration (Γ^*) of electroactive Mb was 1.41×10^{-9} mol cm^{-2}. Also the redox peak potentials showed linear relationship *vs.* lnυ with the equations as Epc(V)=-0.022lnυ (V s^{-1})-0.32 (n=10, γ=0,997) and Epa(V)=0.019lnυ (V s^{-1})-0.19 (n=10, γ=0.995) (Fig. 4C). Then electrochemical parameters of Mb were got by using Laviron's equations [19] with the electron transfer coefficient (α) and the apparent heterogeneous electron transfer rate constant (k_s) as 0.47 and 1.33 s^{-1}. This k_s is higher than former reported values of Mb on C$_{60}$-multiwalled CNT based electrode (0.39 s^{-1}) [20], Ag-CNTs modified glassy carbon electrode (GCE) (0.41 s^{-1}) [21], NiO nanoparticle modified GCE (0.34 s^{-1}) [22], Co nanoparticle modified CILE (0.588 s^{-1}) [23], GR-Pt modified CILE (0.584 s^{-1}) [24] and HSG-SN-CNTs modified GCE (0.41 s^{-1}) [25]. Therefore the electron transfer rate of Mb was accelerated on G-COOH modified electrode due to its high conductivity.
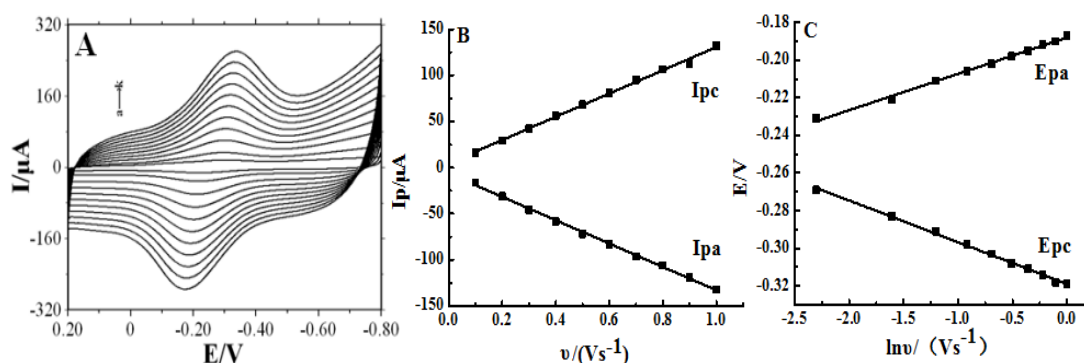

Figure 4. (A) Cyclic voltammograms of Nafion/Mb-G-COOH/CILE in pH 6.0 PBS with different scan rates (a–k: 40, 100, 200, 300, 400, 500, 600, 700, 800, 900, 1000 mV s^{-1}); (B) Linear relationships of redox peak current versus scan rate; (C) Linear relationships of redox peak potential against lnυ.

3.5 Influence of buffer pH

The pH effect can influence the redox peak potential of Mb electrochemistry. As shown in Fig.5A, increasing of pH of the electrolyte from 2.0 to 7.0 resulted in a linear negative shift of E$^{0'}$ with a slope value of -41.77 mV pH^{-1} (Fig. 5B). Although the slope (-41.77 mV pH^{-1}) was smaller than the theoretical value (-59.0 mV pH^{-1}), the electrode reaction could be deduced as a one-proton and one-electron transfer process.
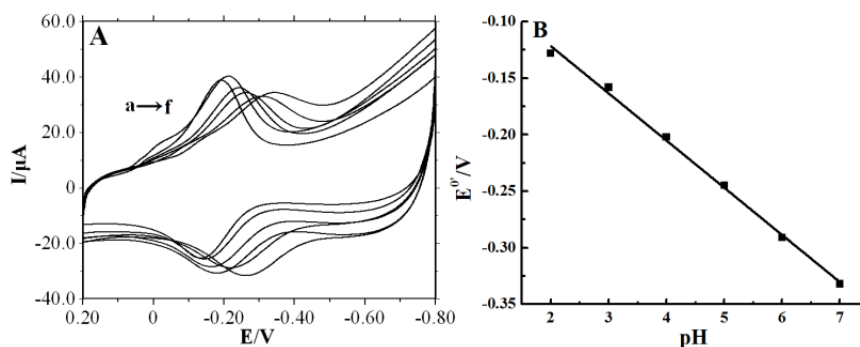
Figure 5. (A) Cyclic voltammograms of Nafion/Mb-G-COOH/CILE in different pH PBS (a-e:2, 3, 4, 5, 6, 7) at the scan rate of 100 mV s^{-1}; (B) Linear relationships of E$^{0'}$ with buffer pH.

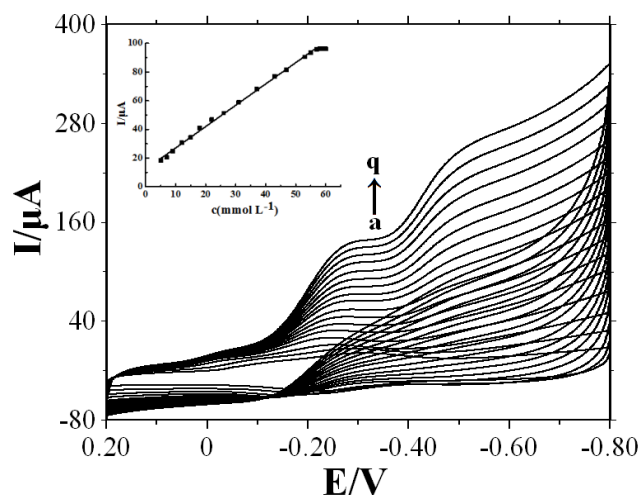*3.6 Electrocatalytic activity*

Figure 6. Cyclic voltammograms of Nafion/Mb-G-COOH/CILE in the presence of different concentration of TCA (a-q: 0.0, 1.0, 1.8, 3.0, 5.0, 7.0, 9.0, 12.0, 15.0, 18.0, 22.0, 26.0, 31.0, 37.0, 43.0, 47.0, 57.0 mmol L^{-1}) at the scan rate of 100 mV s^{-1}. Inset was the linear relationship of catalytic reduction peak currents and the TCA concentration.

Mb film modified electrodes have good electrocatalytic activity to the reduction of organohalides with the decrease of activation energy due to its mimic peroxidase structure. Therefore electrocatalytic reduction of TCA on Nafion/Mb-G-COOH/CILE was investigated by cyclic voltammetry with the data shown in Fig. 6. The increase of TCA concentration led to the increase of reduction peak current at -0.292 V with the decrease of the oxidation peak current (curves a to q), showing the electrocatalytic reduction for TCA. The catalytic reduction peak current had a linear relation with TCA concentration from 5.0 to 57.0 mmol L^{-1} and the regression equation was Iss (μA) =1.48C (mmol L^{-1})+12.26 (n=15, γ=0.998) with the detection limit as 1.0 mmol L^{-1} (3σ). At higher TCA concentration the catalytic peak current reached a stable value and represented a Michaelis–Menten model. Then the apparent Michaelis–Menten constant (K_M^{app}) was got as 1.30 mmol L^{-1} based on the electrochemical version of the

Lineweaver–Burk equation [26]. This value was lower than that of 15.47 mmol L^{-1} on Nafion/Au/GR/CILE [27], 10.67 mmol L^{-1} of Nafion/Mb/NiO/GR/CILE [28], 8.99 mmol L^{-1} of CTS-CTS-GR-IL/CILE [29], 15.78 mmol L^{-1} on IL-LDH/CILE [30] and 1.895 mmol L^{-1} on CTS/Mb/ZrO$_2$/GR/CILE [31], which suggested that Mb immobilized with G-COOH/CILE had high bioactivity and high biological affinity to TCA.

3.7 Analytical application

The analytical application was checked by the determination of TCA content in laboratory water samples with results summarized in table 1 with no TCA residues found in water sample solution. The recovery was verified by standard addition method with TCA standard solution, which was in the range from 101.00% to 103.70% with the relative standard deviation (RSD) value less than 5%.

Table 1. Detection results of TCA in the water sample (n=3).

Water Sample	Found (mmol L^{-1})	Added (mmol L^{-1})	Found (mmol L^{-1})	Recovery (%)	RSD (%)
1	0	6.00	6.22	103.67	3.25
2	0	8.00	8.08	101.00	2.90
3	0	10.00	10.37	103.70	3.02

3.8 Reproducibility and stability

The storage stability of Nafion/Mb-G-COOH/CILE was checked by cyclic voltammetry. 10 days storage at 4 °C refrigerator resulted in the current decreased by 2.6% and 30 days later 95.6% of its original data was remained. The reproducibility of Nafion/Mb-G-COOH/CILE was examined for six parallels detection of 20.0 mmol L^{-1} TCA with RSD of 2.3%, indicating that this modified electrode possessed excellent reproducibility.

4. CONCLUSION

In this study the application of G-COOH on direct electrochemistry of Mb was checked with CILE as the substrate electrode. Direct electron transfer of Mb was realized with a pair of well-defined redox peaks observed on Nafion/Mb-G-COOH/CILE, which was ascribed to the usage of G-COOH with large surface area, good biocompatibility and high conductivity. Also the hydrophilicity made G-COOH solution more stable than GR solution. The immobilized Mb kept its structure after mixed with G-COOH and exhibited excellent electrocatalytic activity to TCA reduction with the advantages such as high sensitivity, wide linear range, low detection limit, long-term stability and good reproducibility.

A comparison of electrocatalytic reduction for TCA detection with some recent reported references was summarized in table 2. Therefore G-COOH could be used for mediator-free electrochemistry of enzymes and the construction of third-generation electrochemical biosensor.

Table 2. Comparison of electrocatalytic TCA analysis with various protein modified electrodes.

Modified electrodes	Linear range (mmol·L^{-1})	Detection limit (mmol·L^{-1})	Refs.
CTS/CMS-Hb/CILE	2.0 - 70.0	0.30	32
CTS/(GR/Mb)$_2$/CILE	0.6 - 26.0	0.15	33
Nafion/Mb-SA-TiO$_2$/CILE	5.3 - 114.2	0.152	34
Nafion/Mb-SA-Fe$_3$O$_4$-GR/CILE	1.4 - 119.4	0.174	35
Nafion/HRP/MoS$_2$/CILE	10.0 - 63.0	0.67	36
CTS/Mb/SWCNHs/CILE	0.9 - 51.0	0.3	37
CTS/NiO-HRP/CILE	0.8 - 38.0	0.26	38
CTS/ Hb-GR-CuS/CILE	1.0 - 64.0	0.20	39
Nafion/Mb-G-COOH/CILE	5.0 - 57.0	1.0	This work

References

1. J. F. Rusling, *Accounts Chem. Res.*, 31 (1998) 363.
2. E. Paleček, J. Tkáč, M. Bartošík, T. Bertók, V. Ostatná and J. Paleček, *Chem. Rev.*, 115 (2015) 2045.
3. S. A. Bhakta, E. Evans, T. E. Benavidez and C. D. Garcia, *Anal. Chim. Acta*, 872 (2015) 7.
4. F. Shi, J. W. Xi, F. Hou, L. Han, G. J. Li, S. X. Gong, C. X. Chen and W. Sun, *Mat. Sci. Eng. C-Mater.*, 58 (2016) 450.
5. X. L. Wang, L. H. Liu, W. Zheng, W. Chen, G. J. Li and W. Sun, *Int. J. Electrochem. Sc.*, 11 (2016) 1821.
6. V. Mani, B. Devadas, S. M. Chen and Y. Li, *ECS Transactions*, 50 (2012) 35.
7. C. Yang, M. E. Denno, P. Pyakurel and B. J. Venton, *Anal. Chim. Acta*, 887 (2015) 17.
8. J. Liu, Z. Liu, C. J. Barrow and W. Yang, *Anal. Chim. Acta*, 859 (2015) 1.
9. D. A. C. Brownson, D. K. Kampouris and C. E. Banks, *Chem. Soc. Rev.*, 41 (2012) 6944.
10. D. Chen, L. H. Tang and J. H. Li, *Chem. Soc. Rev.*, 39 (2010) 3157.
11. T. Gan and S. S. Hu, *Microchim. Acta*, 175 (2011) 1.

12. W. Sun, X. M. Ju, Y. Y. Zhang, X. H. Sun, G. J. Li and Z. F. Sun, *Electrochem. Commun.*, 26 (2013) 113.
13. Y. Liu, J. Gong, W. P. Wu, Y. T. Fang, Q. Wang and H. Y. Gu, *Sensor. Actuat. B- Chem.*, 222 (2016) 588.
14. K. W. Park and J. H. Jung, *J. Power Sources*, 199 (2012) 379.
15. W. Sun, Y. Y. Duan, Y. Z. Li, T. R. Zhan and K. Jiao, *Electroanal.*, 21 (2009) 2667.
16. P. George and C. Hanania, *Biochem. J.*, 55 (1953) 236.
17. D. M. Byler and H. Susi, *Biopolymers*, 25 (1986) 469.
18. A. J. Bard and L. R. Faulkner, *Electrochemical Methods: Fundamentals and Applications.* Wiley, New York, (1980).
19. E. Laviron, *J. Electroanal. Chem.*, 101 (1979) 19.
20. H. Zhang, L. Z. Fan and S. H. Yang, *Chem. Eur. J.*, 12 (2006) 7161.
21. C. Y. Liu and J. M. Hu, *Biosens. Bioelectron.*, 24 (2009) 2149.
22. A. B. Moghaddam, M. R. Ganjali, R. Dinarvand, S. Ahadi and A. A. Saboury, *Biophys. Chem.*, 134 (2008) 25.
23. W. Sun, X. Q. Li, P. Qin and K. Jiao, *J. Phys. Chem. C*, 113 (2009) 11294.
24. W. Sun, L. F. Li, B. X. Lei, T. T. Li, X. M. Ju, X. Z. Wang, G. J. Li and Z. F. Sun, *Mat. Sci. Eng. C-Mater.*, 33 (2013) 1907.
25. C. Y. Liu and J. M. Hu, *Biosens. Bioelectron.*, 24 (2009) 2149.
26. R. A. Kamin and G. S. Wilson, *Anal. Chem.*, 52 (2002) 1198.
27. G. N. Li, T. T. Li, Y. Deng, Y. Cheng, F. Shi, W. Sun and Z. F. Sun, *J. Solid State Electr.*, 17 (2013) 2333.
28. W. Sun, S. X. Gong, Y. Deng, T. T. Li, Y. Cheng, W. C. Wang and L. Wang, *Thin Solid Films*, 562 (2014) 653.
29. C. X. Ruan, T. T. Li, Q. J. Niu, M. Lu, J. Lou, W. M. Gao and W. Sun, *Electrochim. Acta*, 64 (2012) 183.
30. T. R. Zhan, Y. Q. Guo, L. Xu, W. L. Zhang, W. Sun and W. G. Hou, *Talanta*, 94 (2012) 189.
31. W. C. Wang, X. Q. Li, X. H. Yu, L. J. Yan, B. X. Lei, P. Li, C. X. Chen and W. Sun, *J. Iran. Chem. Soc.*, 13 (2016) 323.
32. W. C. Wang, L. J. Yan, F. Shi, X. L. Niu, G. L. Huang, C. J. Zheng and W. Sun, *Sensors-Basel*, 16 (2015) 6.
33. W. C. Wang, X. Q. Li, X. H. Yu, L. J. Yan, Z. F. Shi, X. Y. Wen and W. Sun, *J. Chin. Chem. Soc.*, 63 (2016) 298.
34. H. Q. Yan, X. Q. Chen, Z. F. Shi, Y. H. Feng, J. C. Li, Q. Lin, X. H. Wang and W. Sun, *J. Solid State Electr.*, 20 (2016) 1783.
35. X. Q. Chen, H. Q. Yan, Z. F. Shi, Y. H. Feng, J. C. Li, Q. Lin, X. H. Wang and W. Sun, *Polym. Bull.*, 74 (2017) 75.
36. W. Zheng, G. J. Li, L. H. Liu, W. Chen, W. J. Weng and W. Sun, *Int. J. Electrochem. Sc.*, 11 (2016) 7584.
37. L. J. Yan, X. L. Niu, Z. R. Wen, X. Y. Li, X. B. Li and W. Sun, *Int. J. Electrochem. Sc.*, 11 (2016) 8972.
38. L. J. Yan, X. F. Wang, Q. T. Li, W. C. Wang, S. X. Gong, Z. You, P. Yi and W. Sun, *Croat. Chem. Acta*, 89 (2017) 331.
39. F. Shi, W. Z. Zheng, W. C. Wang, F. Hou, B. X. Lei, Z. F. Sun and W. Sun, *Biosens. Bioelectron.*, 64 (2015) 131.